

Acetaldehyde Chemistry on Ag{111}-(4 × 4)-Ag_{1.83}O between 77 and 200 K Studied by STM

Matthew J. Webb, Stephen M. Driver, and David A. King*

Department of Chemistry, University of Cambridge, Lensfield Road, Cambridge CB2 1EW, UK

Received: September 11, 2003; In Final Form: November 22, 2003

The interaction of acetaldehyde with the Ag{111}-(4 × 4)-Ag_{1.83}O surface oxide structure at temperatures between 77 and 200 K has been studied with scanning tunneling microscopy at 5 K. The bonding sites, relative to the oxide structure, of acetaldehyde at 77 K, and of acetate and ethane-1,1-dioxy formed after annealing to 170 K are discussed. Helical polyacetaldehyde chains formed at 140 K, previously proposed on the basis of RAIRS data, have been observed directly, coexisting with the oxide surface.

Introduction

The partial oxidation of ethene (C₂H₄) to ethene epoxide (C₂H₄O) over silver catalysts has been the focus of considerable study, motivated not least by the industrial importance of this reaction.^{1,2} Much of the debate about the mechanism of epoxidation has centered on the nature of the active oxygen species.^{1,3–6} We have recently investigated this system in detail using a combination of scanning tunneling microscopy (STM), density functional theory (DFT), and STM image simulation.^{7–9} In particular, we have shown that under real catalytic conditions, the active catalyst is likely to be nonstoichiometric silver oxide, and we have determined the site in the oxide structure with which ethene preferentially interacts.

The epoxidation reaction is accompanied by a total combustion reaction, in which acetaldehyde (CH₃CHO) has been implicated as a reaction intermediate.³ On clean metal surfaces, coordination of acetaldehyde to the surface via the O lone pair orbitals results in a weakly bound $\eta^1(\text{O})$ state (Figure 1), which typically desorbs without reaction. This has been observed at low temperatures (<200 K) on Pd{111},¹⁰ Pd{110},¹¹ Ru{001},¹² Cu{111},¹³ and, recently, on clean Ag{111} at 80 K.¹⁴ In the alternative $\eta^2(\text{C}, \text{O})$ state, stronger bonding to the surface occurs through the C=O π orbitals, allowing competitive decomposition processes to take place. On Pd{111},¹⁰ Ru{001},¹² Pt(S){6{111} × {100}},¹⁵ and Ni{100},¹⁶ this has been observed to lead to a mixture of CO, H₂, and hydrocarbon fragments. A recent reflection–absorption infrared spectroscopy (RAIRS) study identified the $\eta^2(\text{C}, \text{O})$ state of acetaldehyde on the oxygen-activated Ag{111} surface at room temperature and high pressures (1 Torr) of ethene or ethene oxide.¹⁷

The study we report here builds on previous work in our group, including a determination of the Ag{111}-(4 × 4)-Ag_{1.83}O structure using a combination of STM, DFT, and STM image simulation,^{7–9,18,19} and a study of acetic acid and acetaldehyde adsorption on this oxide structure using RAIRS.²⁰

The Ag{111}-(4 × 4)-Ag_{1.83}O phase involves a thin oxide film with a hexagonal honeycomb structure, consisting of alternating Ag and O atoms in buckled hexagonal rings forming an O–Ag–O trilayer structure above the Ag{111} substrate. The Ag atoms in the oxide rings have ionic Ag^{δ+} character, and occupy three symmetrically distinct positions denoted

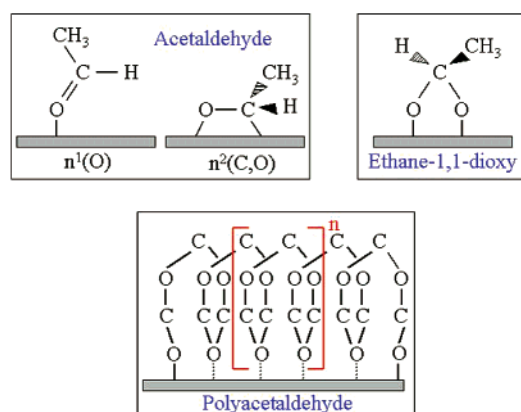


Figure 1. Schematics of the $\eta^1(\text{O})$ and $\eta^2(\text{C}, \text{O})$ states of acetaldehyde, and the bidentate ethane-1,1-dioxy and polyacetaldehyde species. Note that in the diagram of polyacetaldehyde, the H and CH₃ groups attached to each C atom in the polymer chain are omitted for clarity.

Ag₃–Ag₅ in the schematic shown in Figure 2. The rings are centered on 3-fold hollow sites (both fcc and hcp) and atop sites in the underlying substrate; further Ag adatoms, of metallic character, decorate the exposed 3-fold hollow sites (denoted Ag₁ and Ag₂), but not the atop sites (denoted Ag₆). The overall stoichiometry is thus Ag_{1.83}O. The bright features in STM images of the oxide correspond to the metallic Ag₁ and Ag₂ atoms, which themselves define a hexagonal honeycomb of (4 × 4) periodicity; the STM is “blind” to the Ag and O atoms in the oxide rings.¹⁸

In the RAIRS experiments,²⁰ the oxide surface was exposed to saturation doses of acetic acid and acetaldehyde. Acetic acid (CH₃COOH) deprotonates to form acetate (CH₃COO) over the oxide at 240 K, and the resulting RAIR spectra are dominated by the symmetric O–C–O stretch $\nu_s(\text{O–C–O})$ at 1396 cm^{−1}, which was attributed to acetate in a vertical, symmetric bidentate configuration. The acetate was proposed to sit over a bridge site, with its O atoms bonding to adjacent substrate Ag atoms. This geometry was found to be independent of coverage.

In the case of acetaldehyde, the oxide was exposed at 140 K, and then heated progressively to 220 K. At lower temperatures, a series of bands characteristic of the O–C–O vicinal diether linkage (1070–1230 cm^{−1}) were attributed to an acetal species ((RO)₂CHR). On the basis of symmetry arguments, crystalline polyacetaldehyde in a helical chain conformation

* Corresponding author. E-mail: dak10@cam.ac.uk.

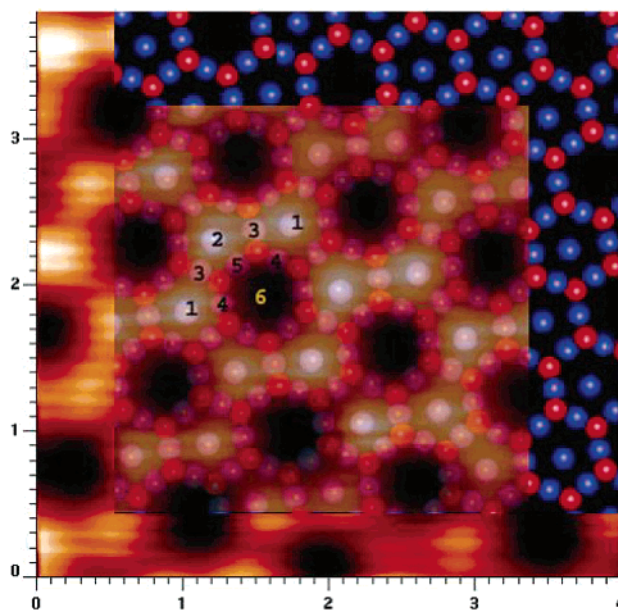


Figure 2. Montage of an STM image ($4 \times 4 \text{ nm}^2$) of the Ag{111}-(4×4)-Ag_{1.83}O surface, and superposed on it a scaled schematic of the structure of this oxide film determined previously (Ag atoms shown in blue, O atoms in red). The numbering scheme Ag_{*n*} used in the text is defined here. Ag₁ and Ag₂ are metallic Ag adatoms in the centers of the rings of the oxide honeycomb, occupying fcc and hcp 3-fold hollow sites above the Ag{111} substrate; Ag₃, Ag₄, and Ag₅ are ionic Ag^{δ+} atoms in the oxide honeycomb; Ag₆ is an exposed Ag atom in the Ag{111} substrate.

(shown schematically in Figure 1) was identified as the most likely candidate. The chain is expected to lie with its axis parallel with the surface, interacting with the surface via the O lone pairs. The degeneracy of E₁ modes of the free polymer would be lifted by the interaction with the surface, accounting for the distinct band-splitting observed in the RAIR spectra. The mechanism of polymerization was suggested to be direct addition of nucleophilic surface atomic O to the aldehyde C=O group to form a surface-bound dioxy fragment: the free O end can then add similarly to the next aldehyde molecule, and so on. Chains formed in this way would be anchored at each end by direct bonding to the surface through the free O atom that terminates the chain.

On heating, the band-splitting attributed to polyacetaldehyde disappears, indicating a reorientation of the polymer chains by rotation about their axes. This is accompanied by conversion to a mix of free acetaldehyde that desorbs, and ethane-1,1-dioxy (CH₃CHOO) in an upright bidentate configuration (shown schematically in Figure 1), which subsequently dehydrogenates to form acetate. The RAIR spectra indicate that these species coexist between 140 and 180 K; by 220 K, acetate is the only remaining species, and it remains stable to ~450 K.

The aim of the STM experiments that we report here was primarily to look for direct evidence of helical polyacetaldehyde chains. However, the STM allows us to work over a wider range of surface temperatures and at lower coverages than were accessible in the RAIRS experiments,²⁰ and we were able to exploit the STM's ability to image single molecules in order to identify preferred adsorption sites of a variety of species on the oxide structure. The RAIRS study suggests a number of species that we might expect to see under different conditions on the surface, including intact acetaldehyde, acetate, ethane-1,1-dioxy and polyacetaldehyde chains. We discuss the interpretation of our STM data in terms of these species in the rest of this paper.

Experimental Details

The Ag{111} crystal was oriented using X-ray Laue diffraction and cut to within 0.5° of the {111} plane before mechanical grinding and polishing (Metal Crystals and Oxides Ltd). After insertion into ultrahigh vacuum (UHV), it was further prepared by cycles of Ar⁺ ion sputtering (1.5 keV, 600 K) and annealing (780 K), until a sharp (1×1) low energy electron diffraction (LEED) pattern and an Auger electron spectrum showing no significant impurities were obtained. At this stage, STM images showed large, clean, and relatively defect-free terraces. Because of the low dissociative sticking probability of O₂ on Ag{111}, the (4×4)-Ag_{1.83}O reconstructed surface was prepared by the procedure of Bare et al.²¹ the clean surface was exposed at 480 K to 600 L (1 L = 10^{-6} Torr s) of NO₂, admitted into the UHV chamber via a leak valve, upon which a (4×4) LEED pattern indicative of oxide formation was obtained. Acetaldehyde (Aldrich, 99%) was degassed by repeated freeze-pump-thaw cycles and its purity verified by mass spectrometry. The oxide surface was exposed at 77 K in the STM chamber to acetaldehyde admitted directly via a pinhole molecular doser. Note that the collimated beam produced by the doser and the cryopumping effect of the cryoshields surrounding the STM mean that a conventional exposure (e.g., in Langmuirs) cannot be determined when dosing in this way.

Experiments were conducted in a UHV system with a base pressure of 1×10^{-10} mbar, housing a low-temperature STM (Omicron Vakuumphysik GmbH) that we have described in detail previously,¹⁹ as well as standard facilities for sample preparation and characterization. The STM itself is attached to the base of a cylindrical bath cryostat and surrounded by cryoshields, allowing operation at 5 K, 77 K, or room temperature. STM imaging was performed with the sample at 5 K or at 77 K, using electrochemically etched polycrystalline tungsten tips. Surface annealing up to room temperature was effected by emptying the cryostats and allowing them to warm. To eliminate the possibility that the surface was affected by other species outgassing from the cryostat walls as they warmed, the surface in each case was prepared in separate experiments by dosing directly at the relevant temperature, allowing us to confirm by STM that the same structures were produced. Surface annealing to temperatures higher than room temperature was achieved by radiative heating in the sample manipulator.

Results and Discussion

1. Acetaldehyde Adsorption at 77 K. The left-hand image in Figure 3 shows an STM image recorded at 5 K of an isolated acetaldehyde molecule adsorbed intact on the Ag{111}-(4×4)-Ag_{1.83}O surface, following a low-coverage exposure at 77 K. A similar image is superposed on a scaled schematic of the oxide structure in the right-hand panel of Figure 3, to allow the registry of the bright feature with the oxide to be readily seen. The feature lies close to the 3-fold Ag-coordinated site defined by the silver atoms Ag₃, Ag₄, and Ag₅, and is slightly elongated in such a way as to partially overlap the neighboring Ag₁₋₂ silver atom.

On clean metals, acetaldehyde typically adsorbs in either the $\eta^1(\text{O})$ or the $\eta^2(\text{C}, \text{O})$ state shown schematically in Figure 1.¹⁰⁻¹⁶ The STM data alone do not allow us to uniquely identify this species as either the $\eta^1(\text{O})$ or the $\eta^2(\text{C}, \text{O})$ state, and at present there is no RAIRS data available for intact acetaldehyde adsorbed on the oxide at 77 K. However, we suggest that this species is more likely to be in the $\eta^1(\text{O})$ state, on the basis that certain aspects of the STM imaging are consistent with its rather weak bonding to the surface. The protrusion is relatively large,

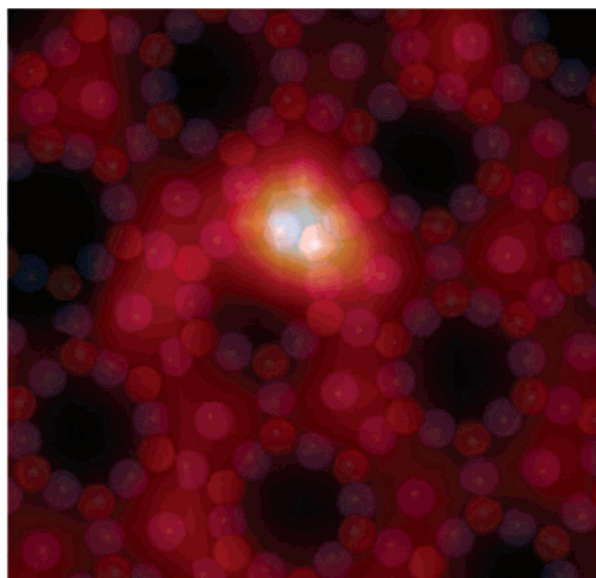
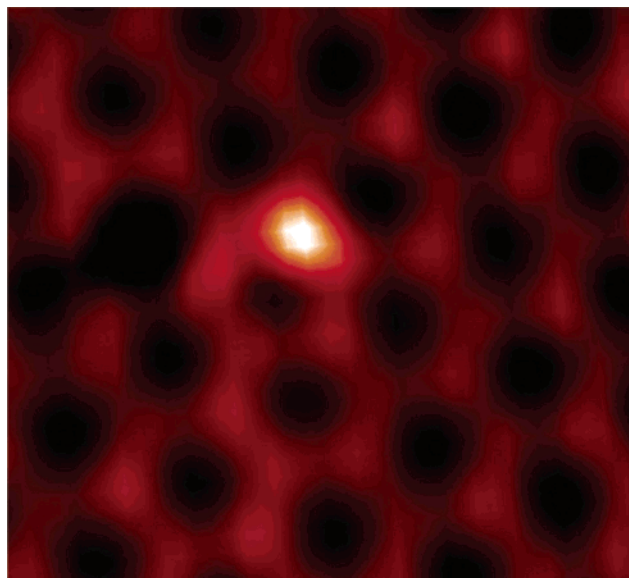


Figure 3. STM images, recorded at 5 K, of an isolated acetaldehyde molecule after adsorption at 77 K on the Ag{111}-(4 × 4)-Ag_{1.83}O surface. The left-hand panel (7.5 × 7.5 nm²) shows a topographic image; the right-hand panel (5 × 5 nm²) shows a current image, and is superposed on a scaled schematic of the oxide structure (color code as for Figure 1). (Sample bias 0.03 V, tunneling current 0.29 nA.)

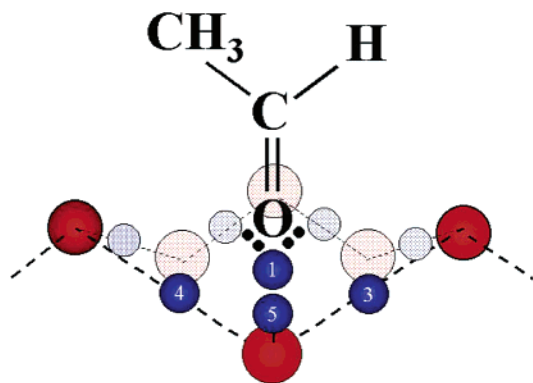


Figure 4. Schematic of proposed model for $\eta^1(\text{O})$ state of acetaldehyde on Ag{111}-(4 × 4)-Ag_{1.83}O surface. The carbonyl oxygen atom is located over the 3-fold site defined by oxide Ag atoms Ag₃, Ag₄, and Ag₅ (blue).

and images recorded at 77 K are somewhat streaky, which may be due to motion of the molecules under the STM tip. In fact, clusters are seen in images recorded at higher coverage immediately after dosing at 77 K, implying significant mobility and attractive interactions of the adsorbed species leading to aggregation, and these clusters tend to be disrupted by the tip as it scans over them. By comparison, images of the more strongly bound ethane-1,1-dioxy species obtained after annealing to 140 K (see below) are considerably less streaky.

This interpretation is in no way contradicted by the observation by Stacchiola et al. of the $\eta^2(\text{C}, \text{O})$ state of acetaldehyde on the oxygen-activated silver surface.¹⁷ Their observations were made at 300 K and 1 Torr, and the fact that they obtained the $\eta^2(\text{C}, \text{O})$ state under conditions very different from ours is a further reason to argue that our images show the $\eta^1(\text{O})$ state.

Our suggested model for this species is therefore based on the $\eta^1(\text{O})$ state of acetaldehyde. In this model, shown in Figure 4, the O atom in the carbonyl group is located over the 3-fold site defined by the ionic oxide Ag^{δ+} atoms Ag₃, Ag₄, and Ag₅, to which coordination of the lone pairs of the carbonyl oxygen is favorable. The orientation of the methyl and hydrogen groups is debatable, but the simplest assumption, that the elongation of the protrusion is parallel to the CH₃-C bond, suggests that the methyl group lies broadly over Ag₄ but slightly displaced

toward Ag₁. The fine detail of this model—especially the C=O bond orientation (on clean Ag{111}, RAIRS indicates that the substrate-O bond is upright and the C=O bond tilted¹⁴) and the position of the methyl group—is necessarily speculative, and amplification from DFT and STM image simulation would clearly be valuable. However, the STM data do allow us to make two firm deductions: the approximate position relative to the oxide structure at which the acetaldehyde preferentially adsorbs, and the fact that the oxide film remains essentially intact.

2. Structures Formed after Annealing: Dependence on Coverage

Acetate and Ethane-1,1-dioxy Monomers at Low Coverages. The STM image in Figure 5, recorded at 77 K, shows a typical area of the surface after exposure at 77 K to a sub-saturation dose of acetaldehyde followed by annealing to 170 K. Three distinct types of feature, labeled A, B, and C, can be seen. Much of the streaky noise characteristic of images of acetaldehyde at 77 K is absent in images recorded after annealing, implying stronger bonding of the resulting species.

We attribute feature A, a bright feature decorating the center of a hexagon of Ag₁/Ag₂ atoms, to an acetate (CH₃COO) species located above an Ag₆ atom; some conversion of acetaldehyde to acetate is expected at 170 K, on the basis of the RAIRS data.²⁰ This identification was confirmed by separate experiments in which identical features, as shown in the inset to Figure 5, were obtained after exposing the oxide surface at 200 K to acetic acid (CH₃COOH), which is known to deprotonate at this temperature to form acetate. Note that although A and B features appear to be paired in Figure 5, both types of feature were seen in isolation from each other in other images. Nevertheless, the fact that pairing is sometimes observed may indicate at least a weak attractive interaction between the A and B features.

When acetate is formed by deprotonating acetic acid, both O atoms in the acetate molecule clearly originate in the acetic acid molecule. By contrast, when acetate is formed by conversion of acetaldehyde, the second O atom must be sourced from surface O. One possibility is that the ethane-1,1-dioxy species discussed below dehydrogenates to acetate. However, the molecule might then be expected to stay in the same site, instead

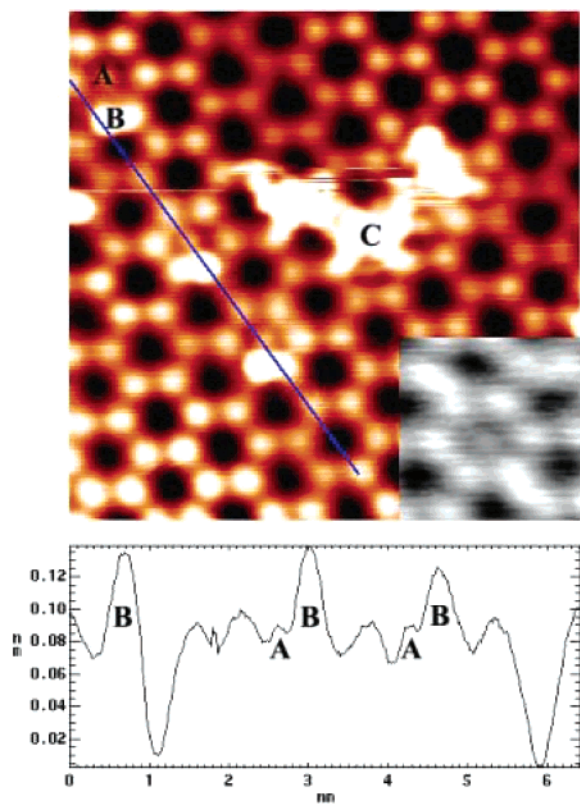


Figure 5. STM image ($7 \times 7 \text{ nm}^2$), recorded at 77 K, of the $\text{Ag}\{111\}$ -(4×4)- $\text{Ag}_{1.83}\text{O}$ surface after a sub-saturation exposure to acetaldehyde followed by annealing to 170 K. The identification of the A, B, and C features as acetate, ethane-1,1-dioxy, and polyacetal aggregates is discussed in the text. A topographic section encompassing A and B features is shown. (0.12 V, 0.46 nA) The inset shows an acetate species produced in separate experiments by deprotonating acetic acid, for comparison to the A features.

of moving to the Ag_6 position. If on the other hand, the molecule moves to the Ag_6 site after conversion to acetate, it must take with it the second O atom, sourced from the oxide (see the discussion below), if it is to remain as acetate. The oxide would then be disrupted, for which we do not see any evidence. Another alternative is that an acetaldehyde can attack an Ag_6 site directly, interacting with an O atom in the adjacent oxide ring and dehydrogenating to acetate. This might be expected to give a different situation to that obtained with an acetate sourced from acetic acid, however, since the molecule must either share the O atom with the oxide, or disrupt the oxide. Clearly this needs further investigation, perhaps using acetaldehyde with isotopically labeled ^{18}O and STM-IETS (inelastic tunneling spectroscopy, which is isotopically sensitive²²). Despite these difficulties, the A features do seem to provide very clear evidence of the presence of acetate.

The most commonly observed species, feature B, differs distinctively from acetaldehyde in its appearance, and we attribute feature B to an ethane-1,1-dioxy monomer. These can be expected to form by means of an acetaldehyde molecule tilting until the carbonyl C atom can interact significantly with one of the upper O atoms (denoted O_u) in the (slightly rumped) hexagonal oxide ring. This disrupts the $\text{C}=\text{O}$ bond and leads to an $\text{O}-\text{C}-\text{O}$ bonding configuration as shown schematically in Figure 6. This would be consistent with the evidence in the RAIRS spectra for an upright bidentate dioxy species, albeit that in the RAIRS study this species was obtained during decomposition of polyacetaldehyde after a saturation dose.²⁰ Although the coverage used here is far smaller than that used in the RAIRS

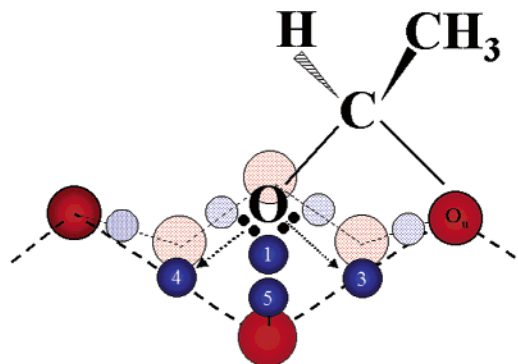


Figure 6. Schematic of proposed model of ethane-1,1-dioxy bonding to the $\text{Ag}\{111\}$ -(4×4)- $\text{Ag}_{1.83}\text{O}$ surface. The carbonyl O is located in a similar way as for acetaldehyde (see Figure 4), but the tilted $\text{C}-\text{O}$ bond allows the carbonyl C to interact with one of the upper O atoms (O_u) in the (buckled) oxide ring. The orientation of the H and CH_3 groups follows from the rehybridization from sp^2 to sp^3 .

study, and would probably be below the sensitivity limit of RAIRS, we infer that band-splitting would be absent if RAIRS spectra could be recorded under these conditions.

The suggested bonding configuration of the ethane-1,1-dioxy species is consistent with the appearance of the B features in the STM images. The feature is elongated, straddles the Ag_1 , Ag_2 , and Ag_3 positions, and appears to be slightly asymmetric (this was found to be independent of scan direction). In the model, the $\text{O}-\text{C}-\text{O}$ linkage lies over the Ag_3 site, and the H and methyl groups point toward the Ag_1 and Ag_2 sites as a result of the sp^3 rehybridization resulting from the formation of the $\text{O}-\text{C}-\text{O}$ linkage. Much of the contribution to the bright feature is thus centered on the carbonyl C and the methyl group, while the positioning of the H and the methyl group accounts naturally for the observed asymmetry.

A key feature of this model is that the O_u atom can be thought of as both a part of the dioxy monomer *and* a part of the oxide ring: thus, as can clearly be seen in the STM image, the oxide structure is not significantly disrupted by dioxy formation. In the RAIRS study, the dioxy was a product of thermal decomposition of polyacetaldehyde chains. The discussion by Sim et al.²⁰ arguably suggests an implicit assumption that surface O is consumed during the polymerization, so that the resulting polyacetaldehyde chains lie above a bare metal surface. By extension, the dioxy decomposition product would be bonded to bare silver as well. The STM data demonstrate clearly that, at least at low coverage, the dioxy must instead be considered to interact with the intact oxide. Strictly, since STM images of the oxide show metallic Ag_1 and Ag_2 atoms but not the ionic Ag_3 , Ag_4 , and Ag_5 atoms in the oxide rings, the STM images only prove that the Ag_1 and Ag_2 atoms remain unaffected. However, we would expect significant disruption of the oxide to lead both to restructuring of the surface and to changes in how the STM images the surface. We therefore believe our conclusion, that the oxide is not disrupted by the dioxy species, to be correct. This in no way contradicts or invalidates the overall interpretation of the RAIRS data, which did not critically depend on the disruption or otherwise of the oxide (and in any case was made before the oxide structure had been characterized).

The identity of the C features is debatable: they may be clusters of unreacted acetaldehyde, or more likely, given the thermal treatment, polyacetaldehyde aggregates.

Self-Organization of Ethane-1,1-dioxy Units. If the acetaldehyde-dosed surface is subjected to a slightly hotter anneal (190 K), linear chain formation is observed, as seen in Figure

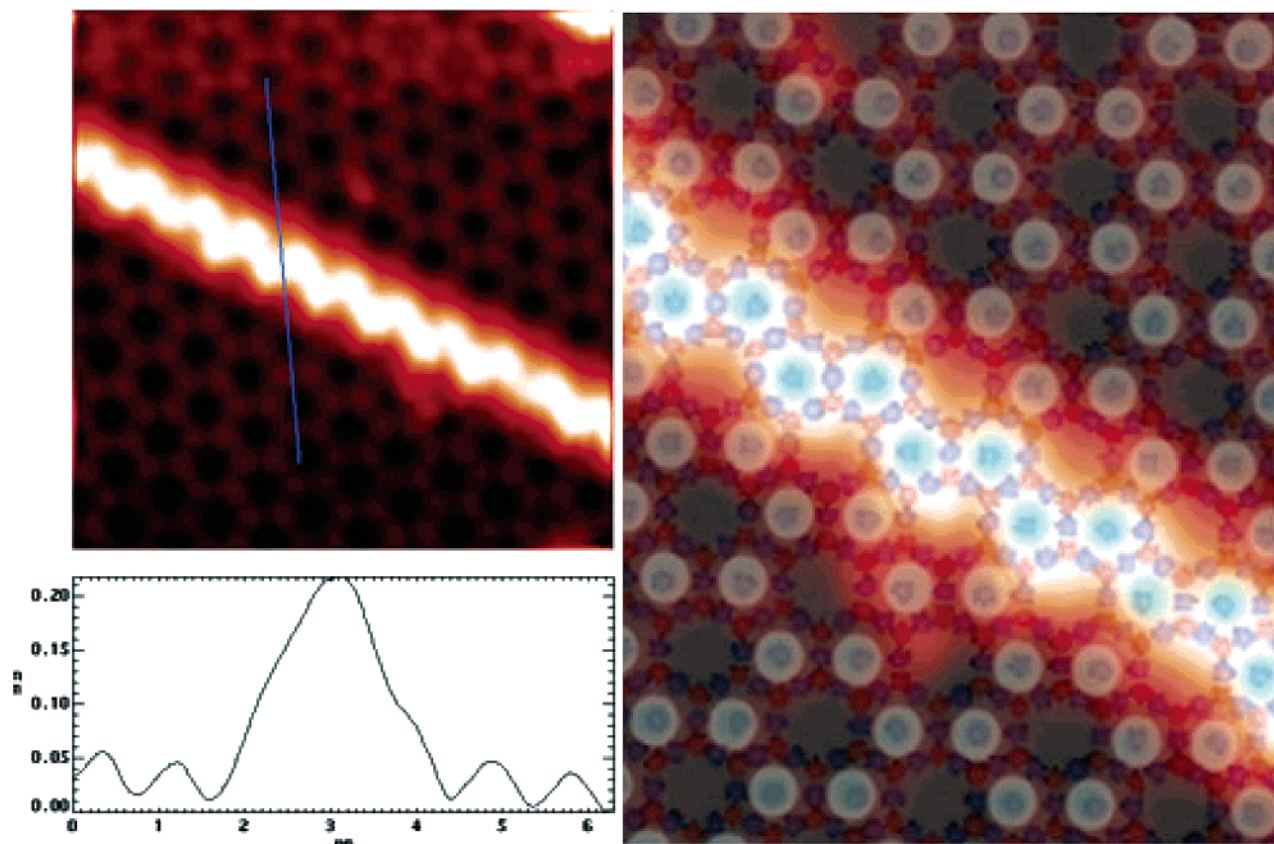


Figure 7. STM images recorded at 5 K showing ordered linear chains above the Ag{111}-(4 × 4)-Ag_{1.83}O surface after a low-coverage exposure at 190 K to acetaldehyde. Upper left: raw topographic image (9 × 9 nm²). Lower left: section through a maximum in the chain. Right: current image (3.3 × 4.9 nm²) superposed on schematic of oxide structure, showing registry. (0.28 V, 0.28 nA)

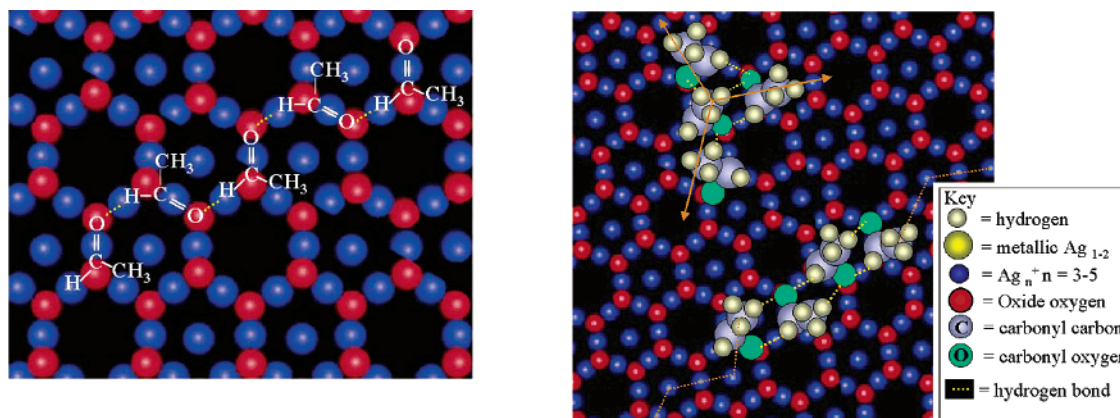


Figure 8. Schematic showing possible structures for the linear chains shown in Figure 7. The left-hand structure involves flat-lying acetaldehyde molecules centered on Ag₃ positions in the Ag{111}-(4 × 4)-Ag_{1.83}O surface and hydrogen-bonding interactions between adjacent members of the chain. The right-hand image (our preferred model) involves intact ethane-1,1-dioxy units. Again, there are hydrogen-bonding interactions between adjacent molecules. (Branched arrangements, as indicated in the upper part of the figure, are also sometimes seen in the STM images.)

7 (left-hand panel). The chains are well ordered, with the maxima along the chain centered over the metallic Ag₁₋₂ atom sites: this can be seen clearly by superposing a schematic of the oxide model (Figure 7, right-hand panel). There is also clearly some enhancement of the apparent heights of the ionic Ag₃ atoms lying between these sites. The maxima have an apparent height ~0.17 nm above the Ag₁₋₂ maxima, as indicated in the section across the chain shown in Figure 7.

The appearance of the images is consistent with a zigzag row of dioxy species, with the O—C—O linkages centered on adjacent Ag₃ sites, shown schematically in Figure 8. Although the driving force for chain formation is unclear, it may be due

to hydrogen-bonding interactions between the carbonyl oxygen and hydrogens attached to the carbonyl carbon and to the methyl groups. This is our preferred interpretation. An alternative possibility involves intact acetaldehyde molecules. By placing the molecules in a flat-lying configuration with the C=O bond located over Ag₃ sites, it is possible to arrive at an arrangement that again permits hydrogen-bonding interactions, this time between the carbonyl O of one monomer and the H group of the next, as shown schematically in Figure 8. The attraction of this model is again that the hydrogen-bonding accounts for the very linear nature of the chains, but against this we note that we would not expect acetaldehyde molecules to remain intact

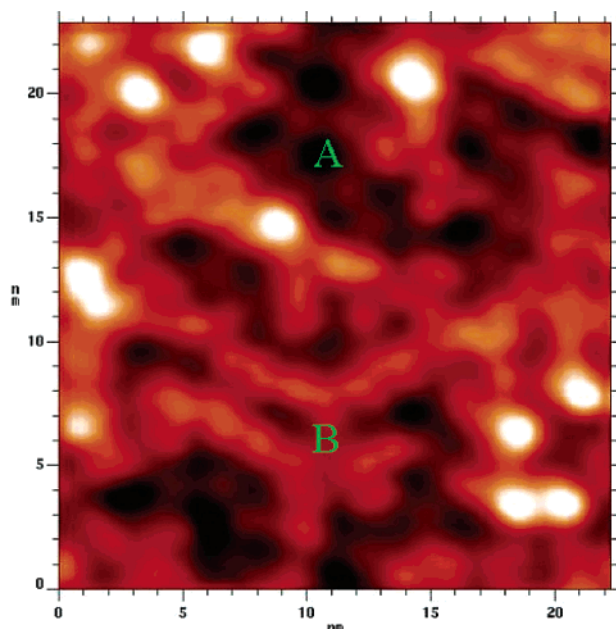


Figure 9. STM image ($22 \times 22 \text{ nm}^2$) of the $\text{Ag}\{111\}-(4 \times 4)\text{-Ag}_{1.83}\text{O}$ surface after exposure at 140 K to effect a moderate coverage of acetaldehyde. The linear features (B) are attributed to polyacetaldehyde chains above the intact oxide structure (A).

after annealing and that it is unclear why the bonding configuration inferred should be different to that discussed above. Clearly further work is needed to understand better the nature of these chains.

We can rule out the other obvious candidate for this structure, polyacetaldehyde chains, on structural grounds. Adjacent maxima in the chain are separated by 6.7 \AA , the spacing of adjacent Ag_{1-2} atoms in the oxide structure. This distance is too great, by nearly 4 \AA , to be consistent with an $\text{O}-\text{C}-\text{O}$ bond in a polyacetaldehyde chain. Moreover, we do see features that we attribute to polyacetaldehyde chains under different conditions, as described below; this gives us further grounds to rule out polyacetaldehyde chains as the origin of the features described here.

Polyacetaldehyde Chains at Intermediate Coverages.

Figure 9 shows an STM image of the surface after exposing the oxide at 140 K to effect a moderate coverage of acetaldehyde. At low coverages, all acetaldehyde molecules have converted at 140 K to ethane-1,1-dioxy, as discussed above; with increasing coverage, we can expect bonding between the monomer units, leading to chain formation. As discussed in the Introduction, RAIR spectra after a saturation dose at 140 K were interpreted in terms of helical polyacetaldehyde chains,²⁰ and we therefore interpret the poorly resolved linear features (labeled B in Figure 9) as the polyacetaldehyde chains. The chains are short, and individual links are not resolved by the STM (in contrast to the dioxy chains discussed in the previous section).

The STM data correspond to subsaturation coverage, and with careful inspection, areas of intact oxide can be clearly seen adjacent to the chains. The chains do not occupy any well-defined position relative to the oxide, beyond a broad tendency to align in the three symmetrically equivalent directions defined by the oxide. This is not surprising, in terms of the model shown schematically in Figure 1. The helical conformation is a consequence of the internal bonding of the polymer chain, and the chain primarily bonds to the surface only at its ends, although some interaction between the surface and adjacent O lone pairs in the chain will occur. No particular registry with the underlying oxide is thus expected.

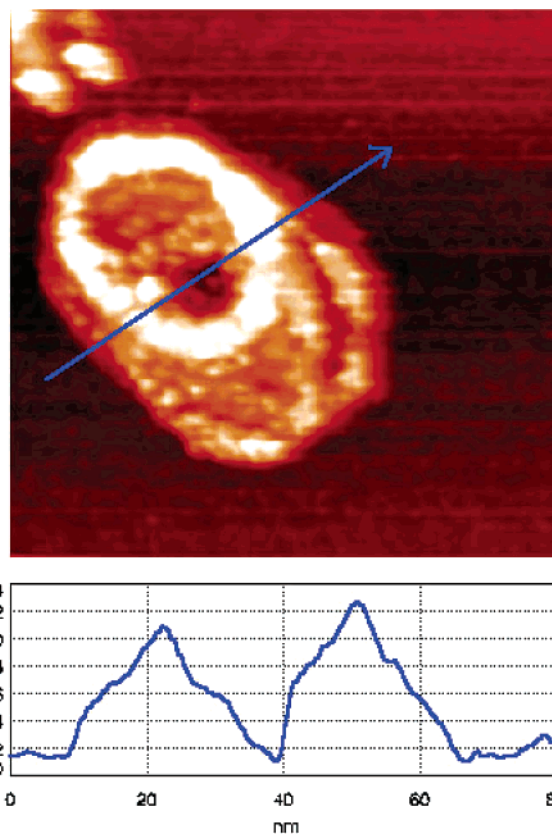


Figure 10. STM image after saturation exposure to acetaldehyde at 140 K, showing a toroidal island.

As mentioned in a previous section, the discussion in the RAIRS study arguably suggests an implicit assumption that surface O is used up in the polymerization such that the chain lies above a clean Ag surface.²⁰ In fact, the proposed polymerization mechanism only requires one surface O per chain, to form the dioxy unit that initiates the polymerization process. Indeed, this is obvious from the schematic model (Figure 1), in which the alternating $-\text{C}-\text{O}-$ structure of the chain is consistent with the simple addition of acetaldehyde monomers without extra O. Thus the appearance of chains in the STM image fully supports the identification by RAIRS of linear polyacetaldehyde chains, while the strong STM evidence that the oxide remains largely intact underneath the chains is completely consistent with the polymerization mechanism proposed in the RAIRS study. It follows that when the polyacetaldehyde chain thermally decomposes to ethane-1,1-dioxy and acetate, as deduced from the RAIRS data, the intact oxide is able to provide the excess O required for dioxy and acetate formation in the way proposed above on the basis of the STM data.

Saturation Coverage: Disorder and Islands. A large dose (1×10^{-7} mbar acetaldehyde at 140 K for 20 min, i.e., $\sim 90 \text{ L}$) leads to multilayer formation. Typical STM images of the saturated surface did not show any ordered structure; the overall measured roughness is $\sim 0.2\text{--}0.25 \text{ nm}$, and the power spectrum retains a degree of 3-fold symmetry consistent with the oxide structure. This rather disordered structure is consistent with RAIRS evidence suggesting a surface of mixed composition at 140 K.²⁰ However, we did frequently observe island features such as that shown in Figure 10.

One possibility is that such features are simply deposits from the STM tip resulting from pulsing the tunneling gap voltage. However, such features were seen in areas in which no such

tip treatment had been applied. Moreover, the features show internal structure that we would not expect to observe in tip-desorption deposits. The edges of the feature are quite pronounced, and concentric lines inside the edges suggest some kind of layered coil structure. The overall height of these toroidal islands is ~ 1.2 nm, and the layers appear to be separated by heights of ~ 0.3 nm.

We suggest that these islands may result from polyacetaldehyde chain growth in a helical conformation, with the axis of the helix approximately perpendicular to the surface, perhaps nucleating at a defect. From an estimation of the volume of a typical island ($\sim 10^6$ Å³) and the effective volume of a single acetaldehyde molecule (of the order of 1 Å³), we can estimate that each island contains $\sim 10^6$ molecules. Thus, despite the wide spacing between them, the islands may account for a significant proportion of the overall coverage.

Conclusions

At low coverage on the Ag{111}-(4 × 4)-Ag_{1.83}O surface at 77 K, we propose that acetaldehyde adsorbs intact in the $\eta^1(\text{O})$ state with the carbonyl O above a 3-fold site defined by ionic Ag₃, Ag₄, and Ag₅ atoms in the oxide honeycomb structure. On annealing to 170 K, the acetaldehyde molecule tilts over until the carbonyl C can interact with an O in the oxide honeycomb to form ethane-1,1-dioxy in an upright bidentate configuration, without disruption of the oxide structure. Some conversion to acetate also occurs. Well-ordered linear chains, which we interpret as comprising ethane-1,1-dioxy monomers, are observed after annealing to 190 K. Following higher-coverage exposure at 140 K, less well-ordered chains are observed, supporting the identification of polyacetaldehyde chains made previously on the basis of RAIR spectra. These are seen to coexist with the intact oxide surface. At the highest coverage, a featureless multilayer surface is seen, together with occasional toroidal islands that we attribute to helical polyacetaldehyde chains coiled above the surface.

Acknowledgment. The authors thank the Engineering and Physical Sciences Research Council for financial support, including a studentship for M.J.W. M.J.W. also thanks Johnson Matthey for financial support. The authors thank W. S. Sim for valuable discussions in the early stages of this project.

References and Notes

- (1) Campbell, C. T. *ACS Symp. Ser.* **1985**, 288, 210.
- (2) Van Santen, R. A.; Kuipers, H. *Adv. Catal.* **1987**, 35, 265.
- (3) Grant, R. B.; Lambert, R. M. *J. Catal.* **1985**, 93, 92.
- (4) Grant, R. B.; Lambert, R. M. *J. Catal.* **1985**, 92, 364.
- (5) Campbell, C. T. *J. Phys. Chem.* **1985**, 89, 5789.
- (6) Campbell, C. T.; Koel, B. E. *J. Catal.* **1985**, 92, 272.
- (7) Michaelides, A.; Bocquet, M.-L.; Sautet, P.; Alavi, A.; King, D. A. *Chem. Phys. Lett.* **2003**, 367, 344.
- (8) Bocquet, M.-L.; Sautet, P.; Cerda, J.; Carlisle, C. I.; Webb, M. J.; King, D. A. *J. Am. Chem. Soc.* **2003**, 125, 3119.
- (9) Bocquet, M.-L.; Michaelides, A.; Loffreda, D.; Sautet, P.; Alavi, A.; King, D. A. *J. Am. Chem. Soc.* **2003**, 125, 5620.
- (10) Davis, J. L.; Barteau, M. A. *J. Am. Chem. Soc.* **1989**, 111, 1782.
- (11) Shekhar, R.; Barteau, M. A.; Plank, R. V.; Vohs, J. M. *J. Phys. Chem. B* **1997**, 101, 7939.
- (12) Henderson, M. A.; Zhou, Y.; White, J. M. *J. Am. Chem. Soc.* **1989**, 111, 1, 1185.
- (13) Lamont, C. L. A.; Stenzel, W.; Conrad, H.; Bradshaw, A. M. *J. Electron Spectrosc. Relat. Phenom.* **1993**, 64–65, 287.
- (14) Wu, G.; Stacchiola, D.; Collins, M.; Tysoe, W. T. *Surf. Rev. Lett.* **2000**, 7, 271.
- (15) McCabe, R. W.; DiMaggio, C. L.; Madix, R. J. *J. Phys. Chem.* **1985**, 89, 854.
- (16) Madix, R. J.; Yamada, T.; Johnson, S. W. *Appl. Surf. Sci.* **1984**, 19, 43.
- (17) Stacchiola, D.; Wu, G.; Kaltchev, M.; Tysoe, W. T. *Surf. Sci.* **2001**, 486, 9.
- (18) Carlisle, C. I.; King, D. A.; Bocquet, M.-L.; Cerdá, J.; Sautet, P. *Phys. Rev. Lett.* **2000**, 84, 3899.
- (19) Carlisle, C. I.; Fujimoto, T.; Sim, W. S.; King, D. A. *Surf. Sci.* **2000**, 470, 15.
- (20) Sim, W. S.; Gardner, P.; King, D. A. *J. Am. Chem. Soc.* **1996**, 118, 9953.
- (21) Bare, S. R.; Griffiths, K.; Lennard, W. N.; Tang, H. T. *Surf. Sci.* **1995**, 342, 185.
- (22) Stipe, B. C.; Rezaei, M. A.; Ho, W. *Science* **1998**, 280, 1732.